

# The potential application of agroforestry residues in the adsorption of aniline

Aplicación potencial de residuos agroforestales en la adsorción de anilina

Perla A. Gonzalez Tineo<sup>1</sup> , Yedidia Villegas Peralta<sup>1\*</sup> , Beatriz Guadalupe González-González<sup>\*</sup> , Edna Rosalba Meza Escalante , Denisse Serrano Palacios 

<sup>1</sup> Departamento de Ciencias del Agua y Medio Ambiente, Instituto Tecnológico de Sonora, 5 de febrero 818 sur col. Centro, CP. 85000 Cd. Obregón, Sonora, México.

<sup>2</sup> Departamento de Biotecnología y Ciencias Alimentarias, Instituto Tecnológico de Sonora, 5 de febrero 818 sur col. Centro, CP. 85000 Cd. Obregón, Sonora, México.

## ABSTRACT

A low-cost activated carbon based on agroforestry residues (AAC) was synthesized and characterized to remove aniline (AN), a health and environmentally toxic substance. The batch adsorption assays were used to assess the effect of contact time (1, 2, 6, 12, and 24 h), pH (2, 4, 6, and 8), and AN concentration (1, 5, and 10 mg/L). The adsorption mechanism of AN on ACC and commercial carbons (GAP and PAC) was evaluated and compared through Langmuir, Freundlich, and Temkin isotherms. The results show that AN removal increases with decreasing pH, reaching a maximum AAC removal capacity of 90 %. AAC resulted in similar efficiency to GAC > 90 % at 1 and 5 mg/L. Langmuir shows the best-fit model reaching an  $R^2$  of 0.98. These models explain that the adsorption mechanism of AN on ACC is homogeneous, and monolayer adsorption occurs, achieving a maximum capacity of 1.20 and 1.16 mg/g for ACC and PAC, respectively, with a possible endothermic mechanism suggested by Temkin. The results showed that AAC could be considered an effective and economical adsorbent in removing the AN.

**Keywords:** Aromatic amine, residues, adsorption mechanism, activated carbon, isotherms.

## RESUMEN

Se sintetizó y caracterizó carbón activado (CAA) de bajo costo a base de residuos agroforestales para la eliminación de anilina (AN), la cual es una sustancia tóxica para la salud y el medio ambiente. Se evaluó el efecto del tiempo de contacto (1, 2, 6, 12 y 24 h), pH (2, 4, 6 y 8) con 1, 5 y 10 mg/L de AN. El mecanismo de adsorción de AN en CAA y los carbones comerciales (CAG y CAP) fue evaluado y comparado con las isothermas de Langmuir, Freundlich y Temkin. Los resultados mostraron que la eliminación de AN aumentó con la disminución del pH, el CAA alcanzó una remoción máxima de 90 %. El CAA resultó en una eficiencia similar al CAG > 90 % a 1 y 5 mg/L. El modelo de Langmuir mostró el mejor ajuste con una  $R^2$  de 0.98. Estos modelos explican que el mecanismo de adsorción de AN sobre CAA es homogéneo, y se produce adsorción en monocapa, alcanzando una capacidad máxima de 1.20 y 1.16 mg/g para CAG y CAP respectivamente, con un posible mecanismo endotérmico sugerido por Temkin. El

CAA podría considerarse un adsorbente eficaz y económico en la eliminación del AN.

**Palabras clave:** Aminas aromáticas, residuos, mecanismos de adsorción, carbón activado, isothermas.

## INTRODUCTION

Aniline (AN) is used widely in industries that manufacture pharmaceuticals, dyestuffs, rubbers, pesticides, plastics, and paints. Due to its extensive industrial use, it is possible to find AN in water bodies and environments such as lakes and rivers, which can even flow into the ocean (Khaniabadi *et al.*, 2016). The estimated annual discharge of AN into water bodies is 30,000 tons by non-regulated discharge (Benito *et al.*, 2017). Therefore, it has become one of the 129 prime concern pollutants, according to the United States Environmental Protection Agency (U.S. EPA) (Basiri *et al.*, 2015). Thus, it is highly necessary to eliminate it from industrial effluents previously to their discharge into the water body (Khoshnamvand and Mostafapour, 2017). Several processes can be used to remove AN from wastewater or water sources, such as biodegradation (Liu *et al.*, 2015), oxidation (Yan *et al.*, 2021), coagulation (Chaturvedi and Katoch, 2020), flocculation (Ahmadi *et al.*, 2017), and adsorption, among others.

The adsorption is the most used due to its high effectiveness on the laboratory or industrial scale (Ahmadi and Kord Mostafapour, 2017b). Adsorption technology has arisen as an eco-friendly solution to removing water pollutants (Srivastava *et al.*, 2021; Deng *et al.*, 2020); these have gained relevance for their high efficiency, environmental friendliness, ease of application, exceptional efficiency, and low cost (Fakhri, 2017; Lu *et al.*, 2017). The most widely used adsorbents include carbon materials, zeolites, and recently, metal-organic frameworks (Huang *et al.*, 2021). Although metal frameworks show excellent adsorption capacities, their synthesis implies high costs (Resasco *et al.*, 2021). Therefore, carbon materials such as activated carbon (ACs) appear as a promising alternative for the removal of pollutants in wastewater due to their well-established properties, low cost, efficiency, and versatility in adsorption processes (Guo *et al.*, 2024; Ghanbarpour Mamaghani *et al.*, 2023).

\*Author for correspondence: Yedidia Villegas Peralta  
e-mail: yedidia.villegas@itson.edu.mx

Received: August 12, 2024

Accepted: September 12, 2024

Published: October 17, 2024

One of the challenges facing the adsorption process is the search for new materials that successfully remove organic contaminants (Zhou *et al.*, 2019). One example is the use of unconventional adsorbents such as natural clay (Iglesias *et al.*, 2013; Padilla-Ortega *et al.*, 2013), or some industrial, agricultural, and forest materials (Bosch *et al.*, 2022; Sharma *et al.*, 2022; Zhu *et al.*, 2021). The agroforestry wastes are known for their wide availability for activated carbon production with some properties such as porosity, capacity of adsorption, and appropriate surface activity (Rosales *et al.*, 2015). Moreover, knowing the removal efficiency offered by various adsorbents is essential. However, it is of utmost importance to describe the affinity between the adsorbate and the adsorbent under determinate conditions at equilibrium (Abin-Bazaine, 2022). All this is possible using mathematical models that predict adsorption behavior; some of the most used equation models are Langmuir (Brazesh, 2021) and Freundlich, which are capable to help determine homogeneous or heterogeneous adsorption processes.

For all the aforementioned, this paper had two principal aims, i) Synthesize and characterize a cheap adsorbent prepared from agroforestry residues, and ii) Evaluate the adsorption mechanism of AN on activated carbon through Langmuir, Freundlich, and Temkin isotherms.

## MATERIAL AND METHODS

### Adsorbent preparation and characterization

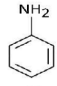
Dried agroforestry residues (mesquite wastes) were mixed with  $H_3PO_4$  solution at 40 % of concentration. The moisture of the residue mixture with the chemical agent was removed in an oven (EHOSELF3-3000 serials) at 105 °C for 12 h. In a muffle (NEY-M325) the dried material was thermally degraded at 400 °C for 2 h and cooled down under ambient conditions in a desiccator (NALGENE, 5312-0230). Subsequently, the obtained agroforestry-activated carbon (AAC) underwent several washes with deionized water to remove the remaining acid. Finally, the ACC was dried at 110 °C all day; the final product was used for characterization and adsorption essays. Physical parameters such as the moisture and ash content of ACC were characterized according to Yokout *et al.* (2015). The analysis for identifying the presence of the different chemical groups for ACC was determined using the Fourier Transformed Infrared Spectroscopy (FTIR), and the accessory used to read the samples was iD1 for diffuse reflectance. The Brunauer-Emmett-Teller (BET) method was followed to determine the superficial area through an advanced analyzer (Quantachrome Autosorb-iQ-C, USA). Commercial Granular Activated Carbon (GAC) and Powdered Activated Carbon (PAC) were also purchased commercially to compare a low-cost adsorbent with an existing one.

### Characteristics of aniline

Aniline was obtained from the effluent of an anaerobic reactor that operated with wastewater from synthetic dyes and which concentration can reach 40 mg/L of AN. Table 1 shows the general characteristics of aniline.

**Table 1.** Properties of aniline.

**Tabla 1.** Propiedades de la anilina.

Parameter	Molecular Weight	$\lambda_{max}$	Molecular Formula	Chemical Structure
Aniline	93.13	198	$C_6H_5NH_2$	 Aniline

Where: Molecular weight (mg/ mol);  $\lambda_{max}$  (nm).

### Adsorption Batch Studies

The adsorption studies were carried out under different AN concentrations (1, 5, and 10 mg/L), contact times (1, 2, 6, 12, and 24 h), and pH (2, 4, 6, and 8). The pH solution was modified according to the necessity by dropping 0.1 N HCL. Each flask in the experiment had a working volume of 100 mL of AN sample that was contacted with 0.5 g of AAC with a stirring (50 rpm). A UV-visible spectrophotometer quantified AN at 198 nm. Equation 1 was used to estimate the removal efficiency.

$$AN R_{em} (\%) = \frac{C_0 - C_1}{C_0} \times 100 \quad (1)$$

Where: AN Rem (%) is the removal efficiency,  $C_0$  (mg/L) is the initial AN concentration, and  $C_1$  (mg/L) is the final concentration of AN.

### Adsorption Isotherms

Several models were suggested for analyzing equilibrium experiments. One of the most important is adsorption isotherms: Langmuir, Freundlich, and Temkin isotherms.

Freundlich isotherm is explaining as an adsorption heterogeneous, considering that exist various sites of adsorption with different quantities of heat energy (Asencios *et al.*, 2022). The linearized equation is:

$$\text{Log } q_e = \text{Log } K_F + \frac{1}{n_F} \text{Log } C_e \quad (2)$$

Where  $q_e$  (mg/g) is the amount of adsorbate that is adsorbed in the adsorbent.  $C_e$  is the concentration (mg/L) of adsorbate in the equilibrium time.  $K_F$  is the constant related to the adsorption capacity (mg/g), and  $1/n_F$  is a constant associated with adsorption intensity.

The Langmuir isotherm is a valid theoretical model for adsorption in a monolayer on a completely homogeneous surface. It has a finite number of identical and specific adsorption sites and negligible interaction between the molecules (Figueroa *et al.*, 2015).

The linearized equation is:

$$\frac{C_e}{q_e} = \frac{1}{q_{max}} C_e + \frac{1}{K_L q_{max}} \quad (3)$$

Where  $q_{\max}$  is the maximum monolayer adsorption capacity (mg/g),  $K_L$  is the Langmuir constant (L/mg),  $C_e$  equilibrium concentration (mg/L), and  $q_e$  is the adsorption capacity at equilibrium (mg/g).

The constant separation factor or equilibrium parameter,  $R_L$ , is a Langmuir isotherm parameter defined by equation 4 (Hall *et al.*, 1996; Webber *et al.*, 1974). The value of  $R_L$  suggests that adsorption can be unfavorable ( $R_L > 1$ ), linear ( $R_L = 1$ ), favorable ( $0 < R_L < 1$ ), or irreversible ( $R_L = 0$ ).

$$R_L = \frac{q_{\max}}{1 + K_L C_0} \quad (4)$$

Where  $C_0$  (mg/L) is the initial dye concentration and  $K_L$  (L/mg) is the Langmuir constant.

Temkin isotherm assumes the heat of adsorption of all the molecules in the layer would decrease proportionally with the increase in the coverage of the adsorbent (Hammed and Rahman, 2008). The linear form of Temkin isotherm is:

$$q_e = \frac{RT}{b_T} \ln K_T + \frac{RT}{b_T} \ln C_e \quad (5)$$

Where  $R$  (8.314 J/mol·K) is the ideal gas constant,  $T$  is the temperature (K),  $b_T$  is the Temkin constant associated with the heat of adsorption (J/mol),  $K_T$  is the equilibrium binding constant (L/g).

### Statistical analysis

The results were expressed as mean  $\pm$  standard deviation, and the isotherm equations were developed using Minitab Statistical 16 and Microsoft Excel software version 16. A regression adjustment was applied to find the best correlation coefficient close to 1.

## RESULTS AND DISCUSSION

### Characterization of adsorbent

The moisture and ash content parameters are important in adsorption efficiency (Tay *et al.*, 2009). According to Castellar *et al.* (2019), the high ash percentage ( $\leq 30\%$ ) would indicate an insufficient activation process. The AAC is in the range of

other ACs (6.5 %). The moisture content of ACs varies widely ranging from 2 % to 90 %, and it is considered that values greater than 15 % decrease the adsorption capability. Finally, the yield parameter is fundamental in terms of costs since it implies the weight of activated carbon per weight of residues utilized for activation. The AAC showed a yield of 50 %, which is higher than others, such as those made from coffee (30 %) or bay leaf (29 %), but lower than that made from coconut (80 %) (Yunus *et al.*, 2022).

### Functional groups (FTIR) and specific surface area (BET)

In Figure 1, the main AAC functional groups are shown. The functional group regions show a broad peak around 3800-3600  $\text{cm}^{-1}$  due to -OH stretching vibrations (Shurvell *et al.*, 2006). The signal at 2361.82  $\text{cm}^{-1}$  is attributed to the C-H stretching vibration (Varghese *et al.*, 2024). The signals in a range of 1300 to 1200  $\text{cm}^{-1}$  were accredited to C=C aromatic stretching; according to the research of Tetteh *et al.* (2024), these bands also can appear in the range of 1600 to 1500  $\text{cm}^{-1}$ . The C-C groups were identified at 1068.68  $\text{cm}^{-1}$ . On the other hand, the bands at 700-900  $\text{cm}^{-1}$  indicated C-H bond vibrations and deformations in aromatic rings (Ghosh, 2020). Additionally, the characterization of the specific superficial area for the AAC resulted in 427.881  $\text{m}^2/\text{g}$ , which was favorable for the adsorption. Commercial activated carbons (PAC and GAC) had a surface area of 800 and 400  $\text{m}^2/\text{g}$ , respectively, according to Carbotecnia <sup>®</sup>. The difference in the surface area values is attributed to the raw material and the use of chemical or physical activation methods (Munoz *et al.*, 2003).

### Morphology SEM analysis

The Agroforestry Activated Carbon (AAC) shows a defined surface morphology represented by ordered fibers, which is presented in the image of SEM 1000 X (Figure 2). The arrangement of the fibers suggests an advantage for adsorption favored by the channels formed between fibers (Brasquet *et al.*, 2020). According to Li *et al.* (2021), the benefits of this kind of arrangement include a large specific surface area, high adsorption rate and capacity, unique surface reactivity,

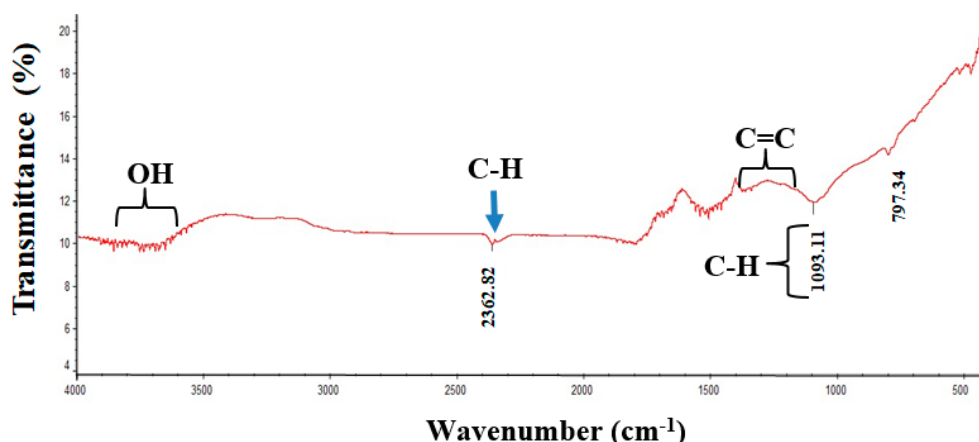


**Figure 1.** FTIR infrared spectrum of Agroforestry Activated Carbon (AAC).

**Figura 1.** Espectro infrarrojo FTIR de carbon activado agroforestal (CAA).

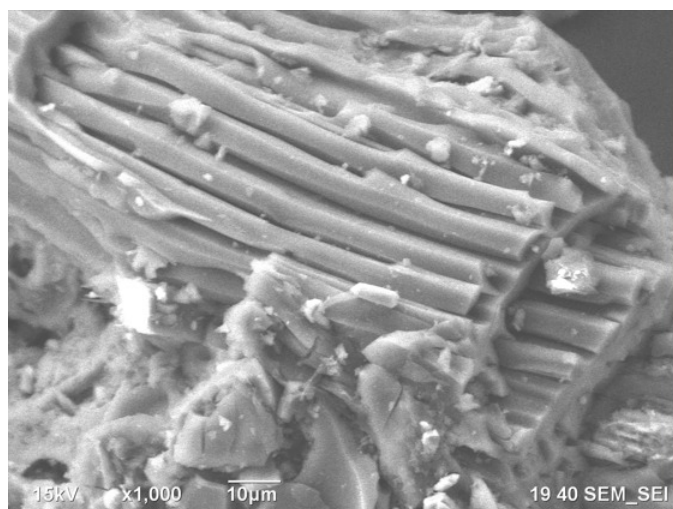


**Figure 2.** SEM image at 1000 X of Agroforestry Activated Carbon (AAC).  
**Figura 2.** Imagen de SEM a 1000 X de carbón activado agroforestal (CAA).

and ease of synthesis. Additionally, Burchell *et al.* (2017), in their study, establish that the large micropore volume of fiber arrangement compared to GAC is the greatest advantage. This can be directly attributed to the fiber structure, which has a very low fraction of closed pores and a large fraction of open pores.

### Effect of pH on the efficiency removal

The pH is a fundamental parameter in the adsorption process (Kord Mostafapour *et al.*, 2016). In Figure 3, this study obtained the maximum removal of AN at acidic pH (2 and 4). In contrast, preliminary analyses indicated that at  $\text{pH} \geq 8$  (results not shown), AN adsorption was not favored. In acidic conditions, the adsorption process increased its efficiency from 52 to  $\geq 80\%$ , and this behavior was similar at each concentration studied, which was 1, 5, and 10 mg/L.

AN is a weak base of an anionic nature that can be transformed into an anilinium ion if it is positively charged under acidic conditions. In this regard, the  $\text{PK}_a$  value of aniline is

4.6, so at acidic pH values, it is positively charged, which increases the  $\text{H}^+$  concentration. Moreover, at alkaline pH, aniline adsorption reduces the competition of other anions, such as  $\text{OH}^-$  (Kord Mostafapour *et al.*, 2016). Sun *et al.* (2021) observed a similar behavior, performing adsorption tests with AC in a pH range between 2 to 12, noting that the adsorption capacity increased in the range of 2 to 5 units, while from pH 5, the capacity decreased by up to 10%. On the other hand, Guo *et al.* (2009) conducted an AN adsorption test with starch-derived compounds; they observed that the adsorption capacities reached the highest value at about pH 4.

### Aniline removal efficiency

The experiment was performed with three different activated carbons: 1) AAC prepared during this study, 2) commercial granular activated carbon (GAC), and 3) powdered activated carbon (PAC). GAC and PAC were purchased to compare a low-cost adsorbent with an existing one on the market.

Table 2 shows that the GAC has removal efficiencies similar to commercial GAC, up to 5 mg/L of AN. On the other hand, one parameter that influenced the adsorption of AN was particle size. PAC used in the tests as a comparison was more efficient than GAC and AAC. At pH 2 and 4 (conditions at which the highest removal was achieved), these carbons showed a removal rate of about 89-90%. Meanwhile, PAC achieved almost 94% removal of AN. The above implies approximately 5% higher. The same situation was repeated at a maximum concentration of 10 mg/L. Wu *et al.* (2013) carried out a study about the effect of particle size on AN adsorption with PAC in five size ranges from 6 to 220; these results showed that AN removal efficiency moderately increased as the particle size decrease, with PAC with powder characteristics obtaining better efficiencies ( $\geq 85\%$ ) at the maximum concentration (10 mg/L).

### Adsorption isotherms

The Langmuir, Freundlich, and Temkin isotherms were studied to define the mechanisms of AN adsorption on AAC and

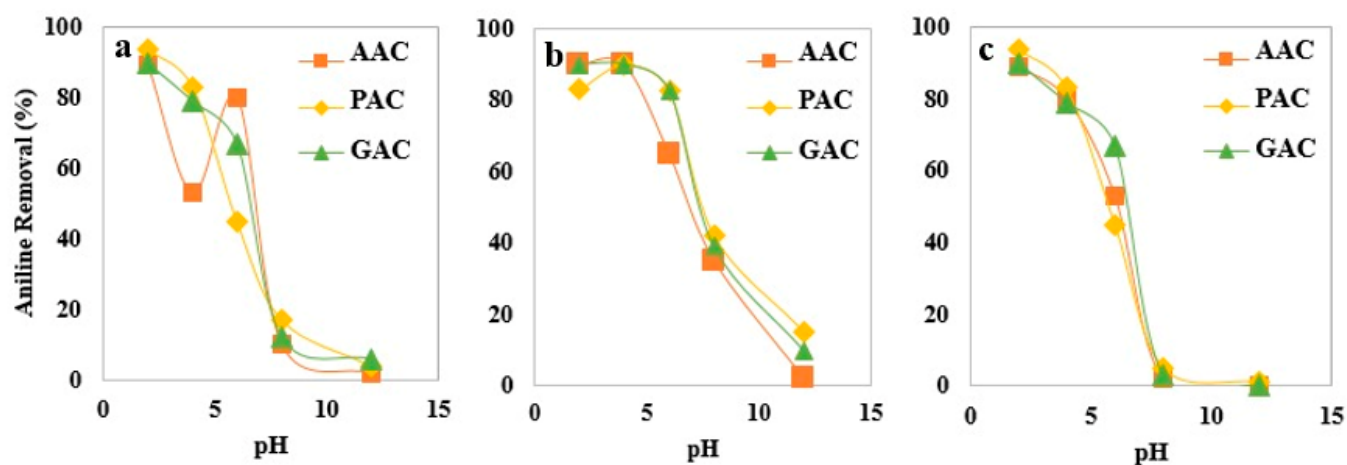


**Figure 3.** Effect of pH on aniline (AN) removal efficiency, at concentrations of a) 1 mg/L, b) 5 mg/L, and c) 10 mg/L.

**Figura 3.** Efecto del pH en la eficiencia de eliminación de anilina (AN) a concentraciones de: a) 1 mg/L, b) 5 mg/L, y c) 10 mg/L.

**Table 2.** Aniline (AN) removal with activated carbon at different pH and concentration.

**Tabla 2.** Remoción de anilina (AN) en carbon activado a diferentes pH y concentración.

Adsorbent	pH	C <sub>0</sub>	C <sub>1</sub>	Removal (%)	Variation coefficient (%)
AAC	6	1.38	0.30	80.00±0.020	9.700
	4		0.65	52.99±0.12	17.76
	2		0.14	89.33 ±0.15	7.640
PAC	6	1.19	0.66	44.68 ± 0.09	13.08
	4		0.2	83.04 ± 0.13	63.98
	2		0.08	93.70 ± 0.01	8.49
GAC	6	1.52	0.5	66.84 ± 0.09	17.96
	4		0.32	79.05 ± 0.02	7.110
	2		0.15	89.79 ± 0.01	0.740
AAC	6	5.34	1.82	65.91 ± 0.091	10.10
	4		Undetectable	>90 ± 0.28	9.40
	2		Undetectable	>90 ± 0.028	12.10
PAC	6	5.91	0.99	82.82 ± 0.14	14.05
	4		Undetectable	>90 ± 0.03	2.7
	2		Undetectable	82.96 ± 0.03	2.7
GAC	6	5.86	1.01	82.76 ± 0.43	9.21
	4		Undetectable	>90 ± 0.52	7.21
	2		Undetectable	>90 ± 1.21	13.23
AAC	6	10.72	6.23	41.88 ± 1.05	18.21
	4		5.54	48.23 ± 1.01	10.54
	2		4.32	59.70 ± 0.98	7.52
PAC	6	9.96	2.70	72.82 ± 0.14	14.05
	4		1.69	82.96 ± 0.03	2.7
	2		0.98	89.96 ± 0.03	2.7
GAC	6	9.11	4.52	50.38 ± 0.52	6.21
	4		2.21	75.74 ± 0.56	5.41
	2		1.33	85.40 ± 0.46	3.21

Where C<sub>0</sub> is the initial concentration of AN (mg/L) and C<sub>1</sub> is the final concentration of AN (mg/L).

commercial activated carbons (PAC and GAC) at equilibrium. Once the experimental conditions for the adsorption process were obtained, they were adjusted to the indicated models. This research shows the fit at AN concentration range of 1 to 10 mg/L and pH 2. Figure 4 shows the result of the determi-

nation coefficient as an indicator of the fit, where the value of the R<sup>2</sup> was 0.9901, 0.94, and 0.99 for PAC, AAC, and GAC, respectively.

Langmuir adsorption isotherm is described by the interaction forces between the adsorbed molecules. Once they occupy a site within the adsorbent, no further adsorption occurs. In this case, the GAC and PAC fit in at a percentage of 99 %, while AAC showed a slightly lower correlation (94 %). The above refers to a homogeneous adsorption process with no in-plane adsorbate transmigration to the surface (Kumar *et al.*, 2007; Foo *et al.*, 2010). The model explains that adsorption takes place in a monolayer and that all sites of the adsorbent material are equal or equivalent. The commercial origin of these carbons can explain this. It can be inferred that PAC and GAC may be structurally similar, so there is no interaction between molecules adsorbed on neighboring sites. When an AN molecule occupies a site in the AC, it is no longer occupied by another molecule of the same origin.

An important parameter for fitting the Langmuir model isotherms is the separation factor (R<sub>L</sub>) (Webber *et al.*, 1974). The R<sub>L</sub> value is useful to define if the adsorption is favorable, linear, not favorable or irreversible. When R<sub>L</sub> is 1, the adsorption is linear; R<sub>L</sub> between 0 and 1 is favorable adsorption; irreversible is when R<sub>L</sub> is equal to 0, while values of R<sub>L</sub> higher than 1 are unfavorable adsorption. In this study, the following values for GAC, PAC, and AAC were of 0.1814, 0.2857, and -1.044, respectively. The above indicates that each studied adsorbent carried out favorable adsorption of AN.

The Freundlich isotherm model assumes that adsorption occurs in multilayer through a non-uniform adsorption distribution on a heterogeneous surface (Hossein *et al.*, 2013). Historically, Freundlich isotherm has been applied for the adsorption of mineral carbon, showing that the percentage of adsorbate in a mass of adsorbent is not constant at different points. In this perspective, the amount adsorbed is the sum of adsorption at all sites (each with a different binding energy), being stronger at the binding sites that are occupied first, until the adsorption energy is exponential and reduces at the end of the adsorption process (Vazquez *et al.*, 2023).

The following images show the fits to the Freundlich models (Figure 5), which were less than 94 % of R<sup>2</sup>.

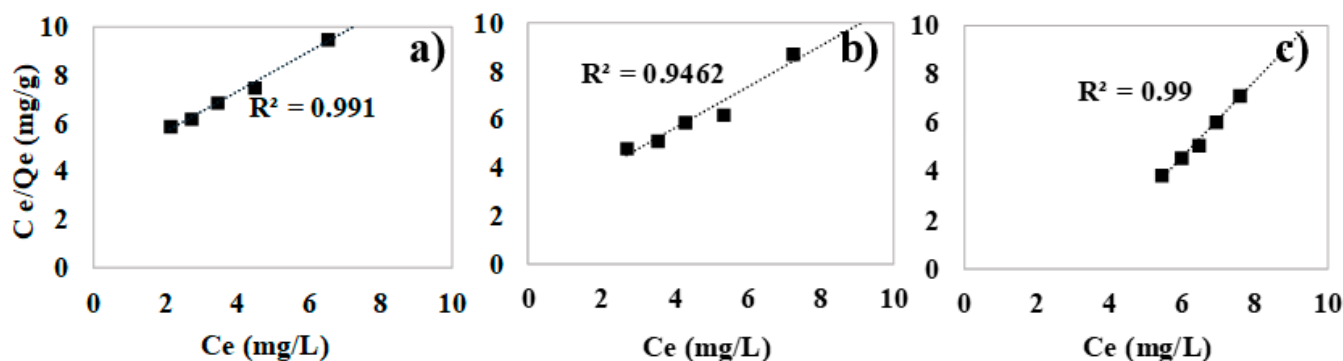


**Figure 4.** Adsorption isotherm with Langmuir model: a) PAC, b) AAC, and c) GAC.  
**Figura 4.** Isoterma de adsorción con el modelo de Langmuir: a) CAP, b) CAA y c) CAG.

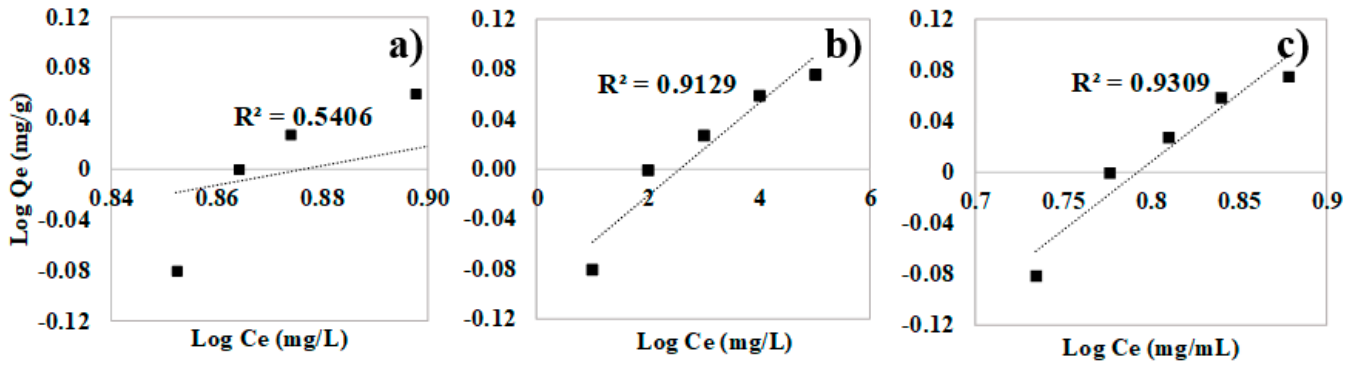


Figure 5. Adsorption isotherm with Freundlich model. a) AAC, b) PAC and c) GAC.

Figura 5. Isoterma de adsorción con el modelo de Freundlich. a) AAC, b) PAC y c) GAC.

According to Figure 5, AAC, PAC, and GAC show a smaller fit to the Freundlich model compared with Langmuir, suggesting a relationship that describes adsorption as a process that is not restricted to forming a multilayer. The results of a similar study reported by Vijan and Neagu (2012), are comparable to those of this work.

The Temkin isothermal model suggests that with increasing surface coverage, the heat of adsorption of all molecules in the layer decreases linearly (Temkin, 1940). The plot of  $q_e$  versus  $\ln C_e$  allowed the isotherm constants  $k_t$  and  $b_T$  to be determined from the intercept and slope, respectively. The Temkin model presented a good fit with an  $R^2$  close to unity for the three carbons evaluated (Figure 6). Therefore, it was one of the two models that best fit the experimental data of this study, both for the system where AAC was used and the commercial ones.

Table 3 shows the parameters of the isotherm mathematical models Langmuir, Freundlich, and Temkin for AN adsorption in AAC, PAC, and GAC. The coefficient of determination ( $R^2$ ) resulting from the Langmuir model for PAC and GAC were similar, with values of 0.9897 and 0.9893, respectively. In the case of ACC, the value of  $R^2$  (0.9462) was lower than the others mentioned before. Considering the model of Freundlich, the  $R^2$  values for ACC, PAC, and GAC were 0.5406, 0.9129, and 0.9309, indicating that the adsorption was not related to a heterogeneous or multilayer way. The model of Temkin resulted in similar values of  $R^2$  compared to Langmuir: 0.9786 for ACC, 0.9754 for PAC, and 0.9792 for GAC.

Table 3. Isotherm parameters for AN adsorption for different activated carbons.

Tabla 3. Parámetros de los isothermas de adsorción para AN para diferentes carbonos activados.

Isotherm model	Parameters	AAC	PAC	GAC
Langmuir	$q_{max}$ (mg/g)	1.1675	1.2070	0.6467
	$k_L$ (L/mg)	0.4510	0.2499	-0.2139
	$R^2$	0.9462	0.9897	0.9893
Freundlich	$k_f$ (mg/g)	0.1414	0.2131	0.8019
	$1/n_f$	0.7657	0.0372	1.0712
	$R^2$	0.5406	0.9129	0.9309
Temkin	$k_t$ (L/g)	0.0039	0.0107	0.0493
	$b_T$ (J/mol)	-8326.6	-7743.9	-2298.2
	$R^2$	0.9786	0.9754	0.9792

The parameter  $q_{max}$  indicates the maximum adsorption capacity for each type of activated carbon studied. It should be noted that PAC is the one that achieved the highest adsorption capacity of 1.2070 mg/g, then ACC with 1.1675, and finally, GAC with 0.6467 mg/g. This is in accordance with the AN removal studies, which show that PAC is the one that achieves the highest removal efficiency with 98 % confidence. Vijan and Neagu (2012) studied the influence

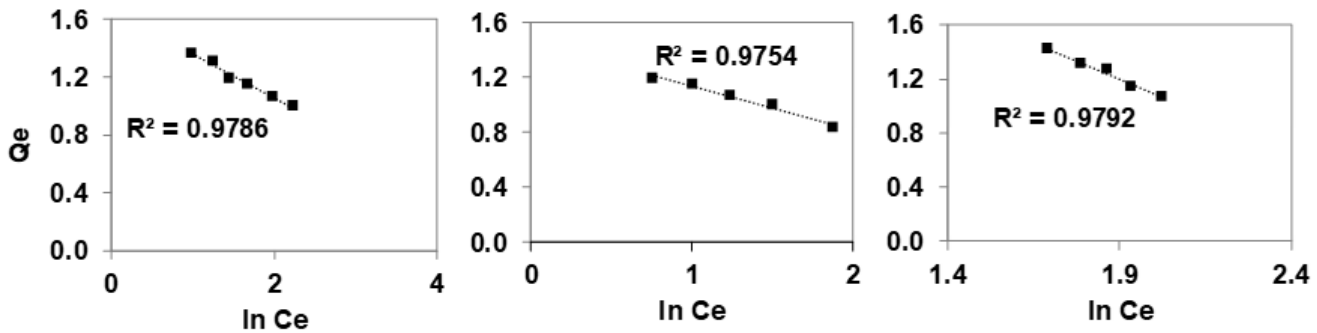


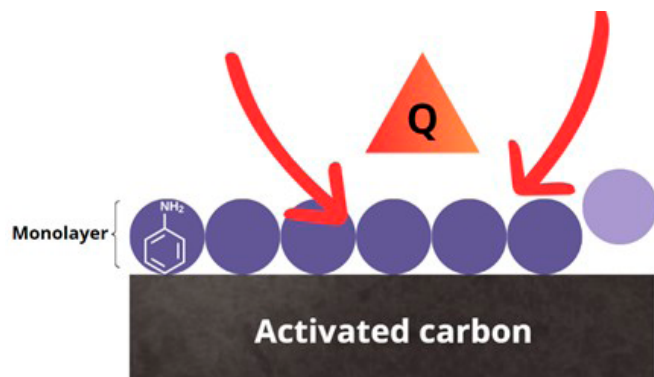
Figure 6. Adsorption isotherm with Temkin model: a) AAC, b) PAC, and c) GAC.

Figura 6. Isoterma de adsorción con el modelo de Temkin Isoterma de adsorción con el modelo de Temkin: a) AAC, b) PAC y c) GAC.

of -OH on activated carbon adsorption; the results of the equilibrium adsorption show that the isotherms were Langmuir type. The same behavior was reported by Santos and Rodrigues (2014), who studied the adsorption equilibrium of aniline onto activated carbon and found that a Langmuir and Bi-Langmuir model was the best representation. It should be recognized that the Langmuir isotherm assumes monolayer adsorption which proposes that there is no interaction between the adsorbed molecules, all of this on a surface with defined adsorption sites and uniform energy.

The utility of the Temkin isotherm is that it allows evaluating the kind of thermic reaction during the process of adsorption. When the constant  $b_T$  results are positive an exothermic adsorption process was developed, by the contrast if a negative value is obtained, the process suggested as endothermic (Benjelloun *et al.*, 2021). The  $k_T$  and  $b_T$  values are shown in Table 3. Similar results were previously reported for activated carbon from *Raphia taedigera* seeds, where an endothermic adsorption process for removing methylene blue was described (Olasehinde *et al.*, 2020).

Figure 7 shows a proposal for aniline mechanism of adsorption on activated carbons. It was inferred that the aniline molecules were adsorbed on activated carbon in a monolayer, favoring the order of the occupied sites in the adsorbent; this fact is related to the Langmuir model with the homogeneous kind of adsorption. The possible mechanism of adsorption was an endothermic nature; it is deduced that the adsorption reaction needs heat to be carried out, which was suggested by the Temkin model.



**Figure 7.** Possible mechanism of aniline adsorption on activated carbon (ACC, PAC, and GAC).

**Figura 7.** Posible mecanismo de adsorción de anilina sobre carbón activado (ACC, PAC y GAC).

## CONCLUSIONS

In this research, agroforestry residues were evaluated for activated carbon synthesis in aniline removal, and the results were compared with two commercial activated carbons: granular and powdered.

Parameters such as pH influenced the adsorption of aniline, which was favored under acidic conditions ( $\leq 4$ ). Instead, the higher the concentration of AN, the lower the removal efficiency of activated carbons. ACC achieved aniline removal efficiencies higher than 90 % when concentrations lower than 5 mg/L of aniline were handled. Furthermore, when the ani-

line concentration was increased to 10 mg/L, the efficiency of the AAC decreased by up to 30 %. The commercial activated carbons maintained their efficiency above 80 % at each concentration evaluated. The efficiency of PAC was higher than GAC and AAC at the maximum concentration of AN and acid conditions (89.96, 85.4, and 59.7 %, respectively). Langmuir and Temkin model isotherm for ACC fitted the adsorption process with an  $R^2$  of 0.94 to 0.99; according to the RL values, the adsorption process was favorable. The above infers that the adsorption process was carried out as a monolayer in a homogeneous manner. Finally, agroforestry residues can be converted into excellent low-cost activated carbons that can economically and safely remove AN and other similar organic compounds without generating more toxic compounds than the original compound.

## ACKNOWLEDGMENTS

The authors wish to acknowledge the financial support of this investigation to the Instituto Tecnológico de Sonora through grant PROFAPI\_2024\_071.

## CONFLICTS OF INTEREST

The authors declared no conflicts of interest.

## REFERENCES

- Abin-Bazaine, A., Trujillo, A.C. and Olmos-Marquez, M. 2022. Adsorption isotherms: Enlightenment of the phenomenon of adsorption. *Wastewater Treatment*, 19, 1-5. doi:10.5772/intechopen.104260.
- Ahmadi S., Kord Mostafapour, F. 2017b. Adsorptive removal of bisphenol A from aqueous solutions by *Pistacia Atlantica*: isotherm and kinetic studies. *Pharm Chem J* 4:1-8. doi.org/10.18801/jstei.050117.35
- Ahmadi, S., Mostafapour, F. and Bazrafshan, E. 2017. Removal of aniline and from aqueous solutions by coagulation/flocculation-flotation. *Chemical Science International Journal*, 18(3), 1-10. doi.org/10.9734/CSJI/2017/32016
- Asencios, Y.J.O., Parreira, L.M., Perpetuo, E.A., and Rotta, A.L. 2022. Characterization of seaweeds collected from Baixada Santista littoral, and their potential uses as biosorbents of heavy metal cations. *Revista Mexicana de Ingeniería Química*, 21(1), IA2600-IA2600. doi.org/10.24275/rmiq/IA2600
- Basiri, H., Nourmoradi, H., Moghadam, F.M., Moghadam, K.F., Mohammadian, J., and Khaniabadi, Y.O. 2015. Removal of aniline as a health-toxic substance from polluted water by aloe vera waste-based activated carbon. *Der pharma chemica*, 7(11), 149-55.
- Benito, A., Penadés, A., Lliberia, J.L., and Gonzalez-Olmos, R. 2017. Degradation pathways of aniline in aqueous solutions during electro-oxidation with BDD electrodes and UV/H<sub>2</sub>O<sub>2</sub> treatment. *Chemosphere*, 166, 230-237. doi.org/10.1016/j.chemosphere.2016.09.105
- Benjelloun, M., Miyah, Y., Evrendilek, G.A., Zerrouq, F. and Lairini, S. 2021. Recent advances in adsorption kinetic models: their application to dye types. *Arabian Journal of Chemistry*, 14(4), 103031. doi.org/10.1016/j.arabjc.2021.103031

- Bosch, D., Back, J.O., Gurtner, D., Giberti, S., Hofmann, A. and Bockreis, A. 2022. Alternative feedstock for the production of activated carbon with ZnCl<sub>2</sub>: Forestry residue biomass and waste wood. *Carbon Resources Conversion*, 5(4), 299-309. doi.org/10.1016/j.crcon.2022.09.001
- Brasquet, C., Rousseau, B., Estrade-Szwarcckopf, H. and Le Cloirec, P. 2000. Observation of activated carbon fibres with SEM and AFM correlation with adsorption data in aqueous solution. *Carbon*, 38(3), 407-422. https://doi.org/10.1016/S0008-6223(99)00120-7
- Brazesh, B., Mousavi, S.M., Zarei, M., Ghaedi, M., Bahrani, S. and Hashemi, S.A. 2021. Biosorption. In *Interface Science and Technology*, (33), 587-628. Elsevier. doi.org/10.1016/B978-0-12-818805-7.00003-5
- Burchell, T.D., Contescu, C.I., and Gallego, N.C. 2017. Activated carbon fibers for gas storage. *Activated Carbon Fiber and Textiles*, 305-335. doi:10.1016/b978-0-08-100660-3.00012-2
- Castellar-Ortega, G., Mendoza C.E., Angulo M.E., Paula P.Z., Rosso B.M. and Jaramillo C.J. 2019. Equilibrium, kinetic and thermodynamic of direct blue 86 dye adsorption on activated carbon obtained from manioc husk. *Revista MVZ Córdoba*, 24(2), 7231-7238. doi.org/10.21897/rmvz.1700
- Chaturvedi, N.K., and Katoch, S.S. 2020. Remedial technologies for aniline and aniline derivatives elimination from wastewater. *Journal of Health and Pollution*, 10(25), 200302. doi: 10.5696/2156-9614-10.25.200302
- Deng, H., Li, Q., Huang, M., Li, A., Zhang, J., Li, Y., ... and Mo, W. 2020. Removal of Zn (II), Mn (II) and Cu (II) by adsorption onto banana stalk biochar: adsorption process and mechanisms. *Water Science and Technology*, 82(12), 2962-2974. doi.org/10.2166/wst.2020.543
- Fakhri, A. 2017. Adsorption characteristics of graphene oxide as a solid adsorbent for aniline removal from aqueous solutions: Kinetics, thermodynamics, and mechanism studies. *Journal of Saudi Chemical Society*, 21, S52-S57. https://doi.org/10.1016/j.jscs.2013.10.002
- Figuroa, D., Moreno, A., and Hormaza, A. 2015. Equilibrio, termodinámica y modelos cinéticos en la adsorción de Rojo 40 sobre tuza de maíz. *Revista Ingenierías Universidad de Medellín*, 14(26), 105-120.
- Foo, K.Y. and Hameed, B.H. 2010. An overview of dye removal via activated carbon adsorption process. *Desalination and Water Treatment*, 19(1-3), 255-274. doi.org/10.5004/dwt.2010.1214
- Ghosh, R.K., Ray, D.P., Tewari, A., and Das, I. 2021. Removal of textile dyes from water by jute stick activated carbon: process optimization and isotherm studies. *International Journal of Environmental Science and Technology*, 18(9), 2747-2764. doi.org/10.1007/s13762-020-03003-5
- Guo, L., Li, G., Liu, J., Yin, P., and Li, Q. 2009. Adsorption of aniline on cross-linked starch sulfate from aqueous solution. *Industrial & engineering chemistry research*, 48(23), 10657-10663. doi.org/10.1021/ie9010782
- Guo, S., Wang, Z., Wu, S., Cai, Y., Zhang, J., Lou, C., and Zhao, W. 2024. Modification of the adsorption model for the mixture of odor compounds and VOCs on activated Carbon: Insights from pore size distribution. *Separation and Purification Technology*, 339, 126669. doi.org/10.1016/j.seppur.2024.126669
- Hameed, B.H., and Rahman, A.A. 2008. Removal of phenol from aqueous solutions by adsorption onto activated carbon prepared from biomass material. *Journal of hazardous materials*, 160(2-3), 576-581. doi.org/10.1016/j.jhazmat.2008.03.028
- Hosseini, S.K., Hosseini, M.M., Reza, A.M., Hassan, H., Mohammad, T., and Maryam, N. 2013. Pre-concentration and equilibrium isotherm studies of rhodium (III) in environmental water samples. *International Journal of Engineering Practical Research*, 2(4), 148-155.
- Huang, D., Zhang, G., Yi, J., Cheng, M., Lai, C., Xu, P., ... and Chen, S. 2021. Progress and challenges of metal-organic frameworks-based materials for SR-AOPs applications in water treatment. *Chemosphere*, 263, 127672. doi.org/10.1016/j.chemosphere.2020.127672
- Iglesias, O., Fernández de Dios, M.A., Pazos, M., and Sanromán, M.A. 2013. Using iron-loaded sepiolite obtained by adsorption as a catalyst in the electro-Fenton oxidation of Reactive Black 5. *Environmental Science and Pollution Research*, 20, 5983-5993. doi.org/10.1007/s11356-013-1610-4
- Khaniabadi, Y.O., Heydari, R., Nourmoradi, H., Basiri, H., and Basiri, H. 2016. Low-cost sorbent for the removal of aniline and methyl orange from liquid-phase: aloe vera leaves wastes. *Journal of the Taiwan Institute of Chemical Engineers*, 68, 90-98. doi.org/10.1016/j.jtice.2016.09.025
- Khoshnamvand, N., Ahmadi, S., and Mostafapour, F. K. 2017. Kinetic and isotherm studies on ciprofloxacin an adsorption using magnesium oxide nanoparticles. *Journal of Applied Pharmaceutical Science*, 7(11), 079-083. doi:10.7324/JAPS.2017.71112
- Kord Mostafapour, F., Ahmadi, Sh., Balarak, D. and Rahdar, S. 2016. Comparison of dissolved air flotation process Function for aniline and penicillin G removal from aqueous solutions. *J. Hamadan Univ. Med. Sci.* 82(4), 203-209. doi 10.21859/hums-230410.
- Kumar, A., Kumar, S., Kumar, S., and Gupta, D.V. 2007. Adsorption of phenol and 4-nitrophenol on granular activated carbon in basal salt medium: equilibrium and kinetics. *Journal of hazardous materials*, 147(1-2), 155-166. doi.org/10.1016/j.jhazmat.2006.12.062
- Liu, B., Du, C., Chen, J.J., Zhai, J.Y., Wang, Y., and Li, H.L. 2021. Preparation of well-developed mesoporous activated carbon fibers from plant pulp fibers and its adsorption of methylene blue from solution. *Chemical Physics Letters*, 771, 138535. doi.org/10.1016/j.cplett.2021.138535.
- Liu, Y.B., Qu, D., Wen, Y.J., and Ren, H.J. 2015. Low-temperature biodegradation of aniline by freely suspended and magnetic modified *Pseudomonas migulae* AN-1. *Applied microbiology and biotechnology*, 99, 5317-5326. doi.org/10.1007/s00253-015-6399-2
- Lu, D., Xu, S., Qiu, W., Sun, Y., Liu, X., Yang, J., and Ma, J. 2020. Adsorption and desorption behaviors of antibiotic ciprofloxacin on functionalized spherical MCM-41 for water treatment. *Journal of Cleaner Production*, 264: 121644. doi.org/10.1016/j.jclepro.2020.121644.
- Mamaghani, Z.G., Hawboldt, K.A., and MacQuarrie, S. 2023. Adsorption of CO<sub>2</sub> using biochar-review of the impact of gas mixtures and water on adsorption. *Journal of Environmental Chemical Engineering*, 11(3), 109643. doi.org/10.1016/j.jece.2023.109643
- Muñoz, Y., Arriagada, R., Soto-Garrido, G., and García, R. 2003. Phosphoric and boric acid activation of pine sawdust. *Journal*



- of Chemical Technology & Biotechnology: International Research in Process, Environmental & Clean Technology, 78(12), 1252-1258. doi.org/10.1002/jctb.923
- Olasehinde, E.F., Abegunde, S.M., and Adebayo, M.A. 2020. Adsorption isotherms, kinetics and thermodynamic studies of methylene blue dye removal using *Raphia taedigera* seed activated carbon. doi 10.22124/cjes.2020.4279
- Padilla-Ortega, E., Leyva-Ramos, R., and Flores-Cano, J.V. 2013. Binary adsorption of heavy metals from aqueous solution onto natural clays. *Chemical Engineering Journal*, 225, 535-546. doi.org/10.1016/j.cej.2013.04.011
- Resasco, D.E., Crossley, S.P., Wang, B., and White, J.L. 2021. Interaction of water with zeolites: a review. *Catalysis Reviews*, 63(2), 302-362. doi.org/10.1080/01614940.2021.1948301
- Rosales, E., Ferreira, L., Sanromán, M.Á., Tavares, T., and Pazos, M. 2015. Enhanced selective metal adsorption on optimised agroforestry waste mixtures. *Bioresource Technology*, 182, 41-49. doi.org/10.1016/j.biortech.2015.01.094
- Santos, M.P., and Rodrigues, A.E. 2014. Adsorption equilibrium and fixed bed adsorption of aniline onto polymeric resin and activated carbons. *Separation Science and Technology*, 49(3), 335-344. doi.org/10.1080/01496395.2013.852226
- Sharma, G., Sharma, S., Kumar, A., Lai, C.W., Naushad, M., Shehnaz, ... and Stadler, F.J. 2022. Activated carbon as superadsorbent and sustainable material for diverse applications. *Adsorption Science & Technology*, 2022, 4184809. doi.org/10.1155/2022/4184809
- Shurvell, H.F. 2006. Spectra-structure correlations in the mid- and far-infrared. *Handbook of vibrational spectroscopy*. doi:10.1002/9780470027325.s4101
- Srivastava, A., Gupta, B., Majumder, A., Gupta, A.K., and Nimbhorkar, S.K. 2021. A comprehensive review on the synthesis, performance, modifications, and regeneration of activated carbon for the adsorptive removal of various water pollutants. *Journal of Environmental Chemical Engineering*, 9(5), 106177. doi.org/10.1016/j.jece.2021.106177
- Sun, Y., Wang, T., Sun, X., Bai, L., Han, C., and Zhang, P. 2021. The potential of biochar and lignin-based adsorbents for wastewater treatment: Comparison, mechanism, and application—A review. *Industrial Crops and Products*, 166, 113473. doi.org/10.1016/j.indcrop.2021.113473
- Tay, T., Ucar, S., and Karagöz, S. 2009. Preparation and characterization of activated carbon from waste biomass. *Journal of hazardous materials*, 165(1-3), 481-485. doi.org/10.1016/j.jhazmat.2008.10.011
- Temkin, M.I. 1940. Kinetics of ammonia synthesis on promoted iron catalysts. *Acta Physicochimica URSS* 12, 327-356.
- Tetteh, I.K., Issahaku, I., and Tetteh, A.Y. 2024. Recent advances in synthesis, characterization, and environmental applications of activated carbons and other carbon derivatives. *Carbon Trends*, 100328. doi.org/10.1016/j.cartre.2024.100328
- Varghese, S.M., Chowdhury, A.R., Arnepalli, D.N., and Rao, G.R. 2024. Crosslinked hydrogel-derived carbons activated by trace amounts of aqueous potassium carbonate for carbon dioxide adsorption. *Bioresource Technology*, 403, 130851. doi.org/10.1016/j.biortech.2024.130851
- Vázquez-Sánchez, A.Y., Lima, E.C., Abatal, M., Tariq, R., Santiago, A.A., Alfonso, I., ... and Vazquez-Olmos, A.R. 2023. Biosorption of Pb(II) using natural and treated *Ardisia compressa* K. leaves: Simulation framework extended through the application of artificial neural network and genetic algorithm. *Molecules*, 28(17), 6387. doi.org/10.3390/molecules28176387
- Vijan, L.E., and Neagu, M. 2012. Adsorption isotherms of phenol and aniline on activated carbon. *Revue Roumaine de Chimie*, 57(2), 85-93.
- Weber, T.W., and Chakravorti, R.K. 1974. Pore and solid diffusion models for fixed-bed adsorbers. *AIChE Journal*, 20(2), 228-238. doi.org/10.1002/aic.690200204
- Wu, C.D., Zhang, J.Y., Wang, L., and He, M.H. 2013. Removal of aniline and phenol from water using raw and aluminum hydroxide-modified diatomite. *Water science and technology*, 67(7), 1620-1626. doi.org/10.2166/wst.2013.038
- Yakout, S.M., and Ali, M.S. 2015. Removal of the hazardous crystal violet dye by adsorption on corncob-based and phosphoric acid-activated carbon. *Particulate Science and Technology*, 33(6), 621-625. doi.org/10.1080/02726351.2015.1016642
- Yan, Z., Gu, Y., Wang, X., Hu, Y., and Li, X. 2021. Degradation of aniline by ferrous ions activated persulfate: impacts, mechanisms, and by-products. *Chemosphere*, 268, 129237. doi.org/10.1016/j.chemosphere.2020.129237
- Yunus, Z. M., Al-Gheethi, A., Othman, N., Hamdan, R., and Ruslan, N.N. 2022. Advanced methods for activated carbon from agriculture wastes; a comprehensive review. *International Journal of Environmental Analytical Chemistry*, 102(1), 134-158. doi.org/10.1080/03067319.2020.1717477
- Zhou, Y., Lu, J., Zhou, Y., and Liu, Y. 2019. Recent advances for dyes removal using novel adsorbents: a review. *Environmental pollution*, 252, 352-365. doi.org/10.1016/j.envpol.2019.05.072
- Zhu, R., Yu, Q., Li, M., Zhao, H., Jin, S., Huang, Y., and Chen, J. 2021. Analysis of factors influencing pore structure development of agricultural and forestry waste-derived activated carbon for adsorption application in gas and liquid phases: A review. *Journal of Environmental Chemical Engineering*, 9(5), 105905. doi.org/10.1016/j.jece.2021.105905.